FUNDAMENTALS OF TRANSPORT PROPERTIES AND IMPEDANCE SPECTROSCOPY IN CEMENT-BASED MATERIALS

John D. Shane and Thomas O. Mason

Northwestern University, Department of Materials Science and Engineering

ABSTRACT

A fundamental step in predicting the durability of cement-based materials is understanding the relationships that exist between transport properties and microstructure, particularly ionic diffusivity and hydraulic permeability. This is especially true when designing and implementing materials to be used for pavement, as they are often exposed to damaging substances such as chloride-containing deicing salts, seawater, sulfates, and carbonates. This manuscript provides a brief overview of the chemistry and microstructure of cement-based materials, and how they influence the transport properties and hence the durability. Several commonly used measurement techniques will also be reviewed. Additionally, the theory and application of impedance spectroscopy to the measurement of transport properties in cement-based materials will be presented.

1. INTRODUCTION

In spite of our growing understanding of the chemistry and physics of cement-based materials, the infrastructure of the United States continues to degrade at an alarming rate, resulting in the expenditure of billions of dollars for replacement and repair every year. The Federal Highway Administration predicts that for the 20 year period between 1981 and 2000 it will cost in excess of $100 billion dollars for the repair of bridges in the United States alone (*1*). If the fundamental relationships that exist between microstructure and transport properties were better understood, concrete and other cement-based materials could be produced to be more durable, as well as with a more predictable service life.

One of the difficulties in making service life predictions is that cement-based materials have microstructural features that cover at least seven orders of magnitude in size, as shown in Table 1. This makes predicting durability a very complex problem, because a change to the system may affect the microstructure on more than one range of size. For instance, the addition of silica fume to cement paste will affect both the gel and capillary pores by decreasing the volume and connectedness of large pores, while increasing the volume of gel pores (*2*). Therefore, both of these effects would need to be fully understood to determine the influence of silica fume on the microstructure and the transport properties.

2. MICROSTRUCTURAL DEVELOPMENT

2.2 Development of Porosity

2.2.1 Capillary Porosity

Fresh paste is a slurry or suspension of cement particles in water. The water phase becomes the capillary porosity and as hydration proceeds, water is consumed and these pores become filled with solids. The amount of capillary porosity, therefore, is a function of both the water to cement ratio (w/c) and the degree of hydration. The capillary pores are normally classified as having diameters between 10 nm and 10 μm (*3*). As the amount of capillary porosity decreases, the pathways between the pores tend to become more tortuous, decreasing the ability for transport. When the w/c ratio is low (• 0.40), the capillary pores can become depercolated at high enough degrees of hydration, effectively isolating the pores, and drastically reducing the transport properties. When the w/c ratio is higher than 0.70, the pores are unable to depercolate, even at complete hydration, allowing relatively easy transport through the microstructure. Thus, cement-based materials with high w/c ratios often exhibit poor durability.

2.2.1 Gel Porosity

The structure of C-S-H, which is the major product of cement hydration, is thought to be composed of nearly amorphous, clay-like layers of calcium silicates with ions and adsorbed water binding the sheets together (*4*). This is shown in Figure 1, which is a rough schematic of the structure proposed by Powers and Brunauer (*3*). Variability in the local stoichiometry can cause folds and defects in the layered structure leading to the formation of very fine pores with diameters of ~0.5 nm to ~10 nm. This fine porosity leads to an enormous surface area that has been measured by nitrogen BET to be 50 - 200 m^2/gram of C-S-H (*5*). The water in these pores does not behave like the bulk water in the capillary pores, as it does not form menisci, and is strongly adsorbed onto the pore walls. When the water is removed, the layers have no disjoining pressure so that they collapse. This irreversible process leads to a more open pore structure which allows easier transport through the material and reduces durability.

3. DIFFUSION AND RELATED PHENOMENA

Cement-based materials are often placed in contact with aqueous environments that contain ions which will reduce their service life (e.g. sulfates, chlorides, carbonates, etc.). The driving force for the diffusion of these ionic species is the gradient in concentration which exists between the external and internal environments of the cement-based material. Diffusion of chloride is a major concern when a concrete contains steel reinforcement. If chlorides diffuse to the steel in high enough concentrations, the passivating oxide film will be disrupted and active corrosion will be initiated. The critical chloride concentration depends on several factors such as steel composition and pore fluid pH. During active corrosion the steel will corrode quickly, forming voluminous reaction products that not only reduce the strength of the reinforcement, but also place the concrete under tensile forces causing spalling and/or cracking, necessitating the need for repair or replacement.

3.1 Diffusion Measurements

In order to determine the ease by which ionic diffusion occurs in a cement-based material, one of two methods is commonly used. The first, known as the divided diffusion cell test, involves placing a disk of material between two water-filled chambers, as shown in Figure 2 (*6*). (Note that for the divided diffusion cell test, the power supply, ammeter, and electrodes are not present.) In this set-up, a solution of ions of known concentration is placed in one chamber which diffuse through the sample and are measured in the downstream chamber. By plotting the concentration of accumulated ions as a function of time, an effective diffusion coefficient (D) can be calculated. The drawback of this method is the weeks or months necessary for steady-state diffusion to be reached. See reference (*6*) for more details.

The second common method, illustrated in Figure 3, involves completely submerging a specimen in a solution of known concentration (*7*). Normally, all but one side of the sample are sealed with an impenetrable coating (e.g. epoxy) to ensure unidirectional diffusion. After a specified length of time, the sample is removed and the concentration of ions is determined as a function of depth. The extraction of the ions from the sample does not differentiate between chemically bound and free species, and thus provides an apparent diffusion coefficient (D_{app}). Like the divided diffusion cell test, the major drawback of this method is the time involved to make the measurements; some tests requiring a 90 day exposure. This makes it all but impossible to study samples early in hydration. For details of this experiment, the reader is referred to (*8*).

3.2 Electromigration

Because of the long times required to make diffusion measurements, several accelerated tests have been developed. The most popular of these tests, the rapid chloride permeability test, developed by Whiting, relies on a high voltage (60 Volts) to drive ions through a disk of concrete in a specified period of time, usually six hours (see Figure 2) (*7*). The amount of current is then measured and the quality of concrete can be determined qualitatively using Table 2.

There are several disadvantages to this technique. The high voltages can heat poor quality samples and permanently damage their microstructure Also, the data collected is of a qualitative nature and therefore cannot be used to make quantitative service life predictions. Nonetheless, the method is widely used because it is fast and can screen a large number of samples. It has also been adopted as a standard test by the ASTM and AASHTO.

An alternative to the rapid chloride permeability test, described by Detwiler *et al.*, involves an apparatus similar to that shown in Figure 2 (*9*). In this test, the driving voltage is dropped from 60 to 12 Volts, reducing the problems with sample heating and microstructure disruption. Unlike the rapid chloride permeability test, this test has the advantage that it measures the migration of ions directly, thus allowing an effective diffusion coefficient to be calculated. Although faster than

the direct measurement of diffusion, this method is much slower than the rapid chloride permeability test and requires days or weeks to complete.

3.3 Normalized Diffusivity and Conductivity

Diffusion in cement-based materials is governed by the volume and complexity of the porosity, as well as the gradient in concentration of the ions (*10*). Shown in Figure 4 is the cross-section of two ideal samples with equal porosity. The sample on the right has several small, cylindrical pores, while the one on the left has one large pore. If edge effects are ignored, the two samples will have the same diffusion coefficient, as long as the pathlengths are equal.

The tortuosity (τ), which is a measure of the pathlength and constrictivity, will also have an important effect on the diffusivity (*11*). Because of the tortuosity, it is possible to have a difference in the diffusivity for samples with the same porosity. This can be seen schematically in Figure 5, with three representations of identical porosity. The pore on the left has no tortuosity whereas the pore in the middle is more tortuous. Given the longer pathlength, the effective diffusion coefficient for the middle pore will be lower. Similarly, the constriction in the pore on the right will also decrease the diffusivity, relative to the pore on the left.

The equation that shows the effects of both the porosity and the tortuosity is (*11*):

$$\frac{D}{D_o} = \phi \beta \tag{1}$$

Where D is the effective diffusion coefficient, D_o is the intrinsic diffusion coefficient, ϕ is the capillary porosity, and β is the connectivity parameter (inverse of tortuosity).

Equation 1 is often referred to as the normalized diffusivity. According to the Nernst-Einstein equation, the normalized diffusivity is exactly equal to the normalized conductivity (*12*). This implies that conductivity measurements, which are normally easier and faster to perform, can be used to estimate the effective diffusion coefficient of a material. The normalized conductivity is shown in Equation 2, where σ is the conductivity of the bulk sample $(\Omega \cdot cm)^{-1}$ and σ_0 is the conductivity of the pore solution $(\Omega \cdot cm)^{-1}$.

$$\frac{\sigma}{\sigma_o} = \phi \ \beta = \frac{D}{D_o} \tag{2}$$

The value of σ can be determined easily, but the measurement of σ_0 requires the extraction of the pore solution from the sample. This is normally not difficult with young pastes of moderate or high w/c ratios, but high performance concretes with low w/c ratios can be problematic. If a pore solution cannot be extracted, it is often possible to estimate the ionic strength from the original oxide composition of the cement, as described by Taylor (*4*).

3.4 Microstructural Considerations

As cement hydrates, the capillary porosity is reduced and the morphology of the pores becomes more complex. The effect of the change in pore structure is shown in Figure 6, which is a plot of normalized conductivity as a function of time for a type I ordinary portland cement paste with a w/c ratio of 0.5. The normalized conductivity drops about two orders of magnitude. Because the capillary porosity decreases by only a factor of two or three, the connectivity (β) must decrease by more than an order of magnitude.

The ability of the normalized conductivity to determine the microstructural characteristics is also demonstrated by Figure 7, which shows the effect of chemical admixtures on the normalized conductivity of cement pastes (*13*). Three pastes were used in this study: one was accelerated with $CaCl_2$, one was retarded with sucrose, and one was left neat as the control. The normalized conductivity, as measured by impedance spectroscopy, is plotted as a function of the capillary porosity. At equal capillary porosity, the retarded sample has the lowest normalized conductivity while the accelerated paste has the highest. Therefore, there is significant difference in the tortuosity between the retarded (highly tortuous) and accelerated (highly connected) samples. Thus, the use of accelerator results in high connectivity between the pores and produces a low durability material.

4. PERMEABILITY

Permeability plays an important role in the durability of concrete because it controls both the rate of entry and the movement of water through the structure. In fact, Mehta has called permeability the most important factor controlling the extent and rate of sulfate attack (*14*). There are a number of instances where the movement of water is critical to the durability of cementitious materials. For instance, water containing dissolved sulfates, which are often present in groundwater and sewage, can be carried into concrete where it can react with monosulfate to re-form ettringite, causing cracking and premature failure (*15*).

4.1 Direct Measurement of Permeability

The measurement of permeability is performed by determining the rate of fluid flow through a slab of concrete or hardened cement paste. Through the application of Darcy's law, the coefficient of permeability can be calculated from flow rate data (*16*). The permeabilities that are measured for pastes are often on the same order as low-porosity (< 5%) rocks, even though the gel porosity might be as high as 25% of the total specimen volume (*4*). Therefore, it can be concluded that the gel pores do not contribute greatly to the overall permeability. In fact, it has been suggested that the permeability of the C-S-H gel is as low as 10^{-22} m/s (*3*).

Although the measurement of permeability seems to be straightforward, it is not without difficulties. For instance, when cement-based materials are tested, the flow rate through the sample is initially high, but decreases by up to an order of magnitude before equilibrium flow is reached (which can take anywhere from days to weeks (*16*)). Although several theories have been proposed, the reasons for the decrease in flow rate are not well understood. One possible explanation is the blocking of pore throats by microparticles dislodged during the initial influx of water, especially when high driving pressures are used. It has also been suggested that the decrease in flow may be the result of C-S-H swelling, or an osmotic effect that results from the filling of previously empty pore space. Because it takes days or weeks for steady-state flow to be reached, samples will change during the course of the test as the water reacts with unhydrated cement grains or leaches calcium hydroxide (*11*). This makes studying the effect of age on permeability difficult, particularly for young samples.

4.2 Prediction of Permeability (Katz-Thompson Equation)

A number of models have been proposed to predict the permeability in porous materials. Some of them work well for systems such as reservoir rocks, but do not seem to work nearly as well for cementitious materials. The reasons for this are unclear, but probably are a result of their complex pore structure. However, one model that was developed to predict the permeability of reservoir rocks has given encouraging results when applied to cement-based materials.

The following equation was developed by A.J. Katz and A.H. Thompson to determine the permeability of rocks saturated with a single conductive liquid phase (*17*):

$$K_p = c\, d_c^2 \left(\frac{\sigma}{\sigma_o}\right) \tag{3}$$

Where K_p is the permeability (m^2), d_C is the critical pore diameter from mercury intrusion porosimetry (m), (σ/σ_O) is the normalized conductivity of the sample, and c is a constant equal to 1/226.

To predict the permeability of a material using the Katz-Thompson equation, two pieces of experimental information must be known. First is the critical pore diameter (d_C), which Katz and Thompson related to the inflection point in mercury injection measurements. At the inflection point, the mercury is able to percolate through the largest pores that completely traverse the sample. The other required information is the normalized conductivity of the specimen, which was discussed in Section 3.4.

The time required to make these predictions is much shorter and much less labor-intensive than the time required to make permeability measurements, which is the main advantage of the Katz-Thompson equation. Also, unlike permeameters, there is no lower or upper limit of permeability that can be predicted. Once set has occurred, and mercury intrusion experiments can be performed, the permeability of any cement-based material can be predicted.

4.3 Microstructure/Permeability Relationships

The effect of depercolated versus percolated capillary porosity on the permeability of hardened cement paste was demonstrated by Powers *et al.* by examining the coefficient of permeability as a function of w/c ratio (Figure 8) (*18*). As the

w/c ratio increases, eventually the pores become connected (or percolated) providing open pathways through the microstructure for fluid flow, and the permeability increases dramatically.

During the first year of hydration, the pore structure of cement paste changes considerably. Capillary porosity is filled by hydration products and becomes tortuous, and gel porosity increases. The changing microstructure results in an 8-10 order of magnitude decrease in permeability, from one day to one year. This large change can be explained by considering the Katz-Thompson relationship (Eq. 3), and the plot of the log permeability as a function of the log critical pore diameter from mercury intrusion measurements in Figure 9 (*19*). From three days to 20 months, there is a two to three order of magnitude drop in critical pore diameter (the x-axis in Fig. 9). According to the Katz-Thompson equation, this should amount to a four to six order of magnitude drop in permeability. Combining four to six orders of magnitude for d_c^2 and two to three orders of magnitude from the change in σ/σ_0 (see Fig. 6), we can readily account for the eight orders of magnitude drop in permeability (the y-axis in Fig. 9).

Since the original work by Powers, who considered only the effect of the volume of capillary porosity, many factors have been found to influence the capillary pore structure, and therefore the permeability (*20-22*). For instance, if the hydration is accelerated (i.e. by elevated temperatures or by chemical admixtures), the capillary porosity will tend to be more connected, as was shown earlier in Figure 7, and also by Goto and Roy, who studied the effect of curing temperature on the permeability of several neat pastes (*22*). Their pastes had various w/c ratios and were hydrated for 28 days at either 27° C or 60° C. The pastes hydrated at the elevated temperatures had lower capillary porosities, but had permeabilities higher by at least an order of magnitude. Mercury intrusion experiments revealed a secondary pore distribution at large pore diameters for the samples hydrated at elevated temperatures, which was concluded to be responsible for the increase in permeability. This simple experiment demonstrates that the pore structure as well as the pore volume will govern the transport properties.

When aggregate is added to cement paste to form mortar or concrete, there is a tendency for the permeability to increase, even though the aggregates themselves are often inert and impenetrable. Halamickova *et al.* demonstrated that there is a systematic increase in the permeability of mortars mixed with various amounts of sand (0% - 55% by volume) (*23*). This was observed for two w/c ratios and supports the observation that the addition of aggregate increases the susceptibility to hydraulic flow.

It is generally accepted that there is a region of relatively high porosity surrounding each aggregate particle, known as the interfacial transition zone (ITZ), which may be responsible for the increase in permeability (*24*). Alternatively, some researchers believe that microcracks form between the aggregate and cement paste as a consequence of the stresses that build up as a result of chemical shrinkage. Bleeding and segregation around the aggregate particles can also provide pockets of open space, which can increase the permeability. Regardless of the source, the aggregates induce the formation of microstructural heterogeneities which reduce the overall durability of cement-based materials.

Mineral admixtures, such as silica fume, ground granulated blast furnace slag, and fly ash have been used as partial replacements for cement with encouraging results. A relatively small addition of silica fume (10% by weight of cement) and fly ash (35% replacement of cement) can decrease the permeability of concretes significantly. Not only do these materials tend to increase durability, the admixtures themselves are often formed as an industrial byproduct that would otherwise have to be disposed of in a costly and/or environmentally unsound manner.

The reasons for these decreases in permeability are varied and complex, but can be discussed generally in terms of their effect on the pore structure. These mineral admixtures normally have particle sizes smaller than the cement grains and thus improve particle packing which decreases the volume and connectedness of the capillary porosity. Moreover, admixtures with a high silica content (e.g. silica fume), react with calcium hydroxide and water to form more C-S-H gel, via the pozzalonic reaction, decreasing the diameter of the capillary pores.

The addition of these materials will affect the interfacial zone as well. The small particle size will ensure that there is good particle packing around the aggregate, which will reduce the porosity of the interfacial zone (*25*). Also, with admixtures undergoing the pozzolanic reaction, the high concentrations of calcium hydroxide that tend to deposit near the aggregate will be converted to C-S-H which will increase the paste/aggregate bond strength and decrease the capillary porosity in the ITZ, further improving the durability.

5. IMPEDANCE SPECTROSCOPY

Impedance spectroscopy (IS) is a non-invasive, non-destructive technique that has become a valuable tool for studying cement-based materials (*26*). It allows the microstructure of the bulk paste, the corrosion of reinforcement, and possibly the microstructure of the interfacial zone to be studied simultaneously (*27*). One of the great advantages of IS is the ability to

make measurements on samples in their natural, saturated state. That is, the technique does not require the specimen to be dried. Also, the size requirements of the specimens are very flexible, which makes IS a potentially useful technique for in-field testing of structures.

To make IS measurements, a small a.c. signal of known voltage and frequency is applied to a specimen. The gain and phase angle are measured and from this, the real (resistive) and imaginary (capacitive) portions of the impedance (Z) can be determined. This procedure is applied through a wide range of frequencies, typically covering 7-10 orders of magnitude (MHz - mHz). Because many transport phenomena have distinctly different resonant frequencies ($2\pi f = 1/RC$) (e.g. ionic migration in the bulk and electrochemical charge transfer at the electrodes), sweeping through a large range of frequencies will allow the different modes of transport to be deconvoluted for study.

Once the real (Z_{real}) and imaginary (Z_{imag}) portions of the impedance are calculated, they are often plotted as $-Z_{imag}$ versus Z_{real}, in what is known as a Nyquist plot. This allows the different transport mechanisms to be seen graphically, as they often form distinct semi-circular arcs above the Z_{real} axis. Figure 10 shows data for the cement-paste/steel system, which includes both the oxide film and bulk responses. The cusp between the two arcs in Figure 10 (a), where Z_{imag} is at a minimum, occurs exactly at the d.c. bulk resistance of the sample (which is used to calculate the conductivity, σ). The frequency at which Z_{imag} is at a minimum occurs at what is known as the cutoff frequency. Because this frequency changes during hydration and as a result of the addition of admixtures, it cannot be assumed that the frequency used in single frequency a.c. techniques corresponds to the cutoff frequency. That is, single frequency techniques may provide erroneous results. Also, two-point d.c. measurements will give inaccurate results because they measure the value of the polarization resistance of the oxide layer. This problem can be eliminated by making four-point resistance measurements, although extremely large voltages may be necessary for resistive specimens.

Impedance spectroscopy (IS) has several advantages relative to the 90 day ponding test or the rapid chloride permeability test in establishing the diffusivity in concrete. First, it is a virtually instantaneous measurement, a typical spectrum taking only minutes to obtain. Second, since very small perturbation fields and short time intervals are employed, IS measurements do not alter the pore structure of the concrete being studied. Third, there are no upper or lower bounds insofar as diffusivity/conductivity are concerned. Finally, the technique is quite flexible, being applicable over a wide range of mix designs and with various admixtures.

6. CONCLUSION

Cement-based materials are the most widely used materials on Earth, but owing to their inherent porosity, they often degrade at an unacceptable rate. The key to understanding the rate at which these materials decay is determining the relationships that exist between transport properties and microstructure. This will enable the microstructure to be tailored in order to obtain desirable transport properties and therefore improved durability.

Unfortunately, estimating the durability of cement-based materials from diffusion and permeability measurements is inhibited by the time involved in making the necessary measurements. Often a single test can take weeks or months making the testing of young specimens and screening large numbers of samples difficult. Fortunately, there are a number of techniques that can reduce the time needed to make these measurements. If the intrinsic ionic diffusivity (D_O) is known (it is often available in handbooks), the effective diffusion coefficient (D) can be estimated by measuring the normalized conductivity (σ/σ_o) of a specimen and using the Nernst-Einstein equation. Permeability can potentially be estimated using the Katz-Thompson equation, which also relies on the normalized conductivity as well as the critical pore diameter. This technique is currently under further investigation.

Impedance spectroscopy, an a.c. technique that measures the resistive and capacitive components of the impedance of a material, can be used to accurately measure the normalized conductivity. The normalized conductivity can be used to determine characteristics of the microstructure, such as the connectivity (β). It is also a measure of the ease by which ions can migrate through the structure of a porous material. This technique has the advantages of being fast, flexible and non-destructive, insofar as concrete pore structure is concerned.

Table 1: Scale of Microstructural Features in Concrete

Microstructural feature	Scale (meters)
Gel porosity	10^{-9} - 10^{-8}
Capillary porosity	10^{-8} - 10^{-6}
Calcium hydroxide crystals	10^{-6} - 10^{-4}
Small aggregate	10^{-4} - 10^{-2}
Large aggregate	10^{-2}

Table 2: Chloride Penetrability Based on Charge Passed (*28*)

Charge Passed (coulombs)	Chloride Ion Penetrability
>4,000	High
2,000-4,000	Moderate
1,000-2,000	Low
100-1,000	Very Low
<100	Negligible

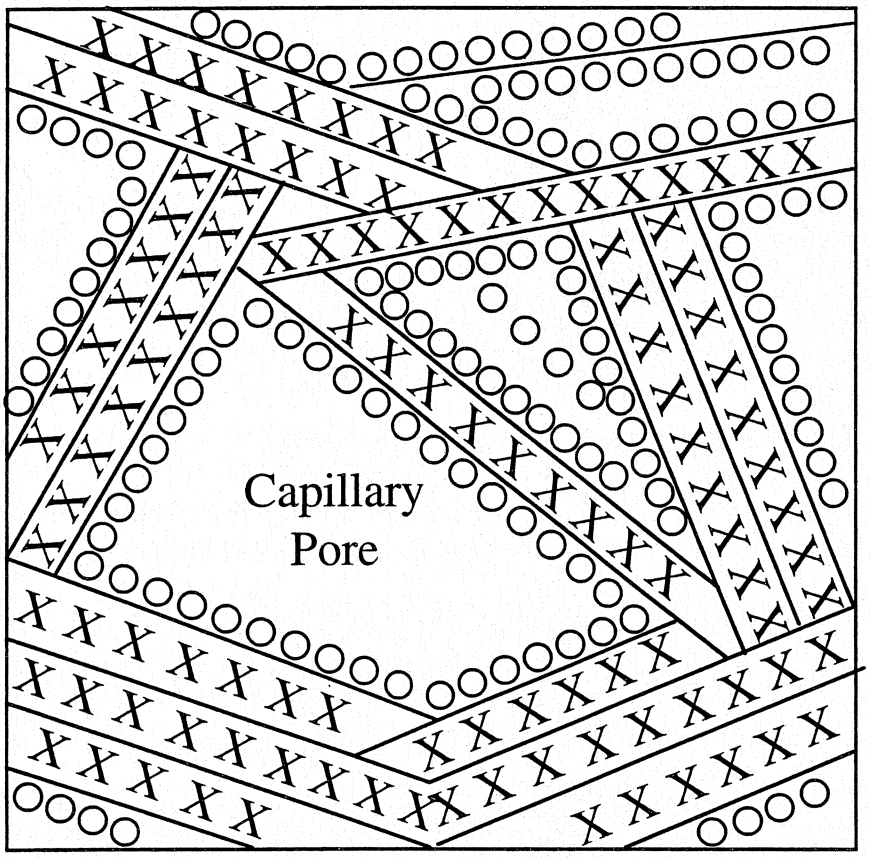


FIGURE 1 A schematic representation of the Powers-Brunauer model of C-S-H. The X's represent water in interlayer regions, the O's represent water adsorbed on surfaces (*3*).

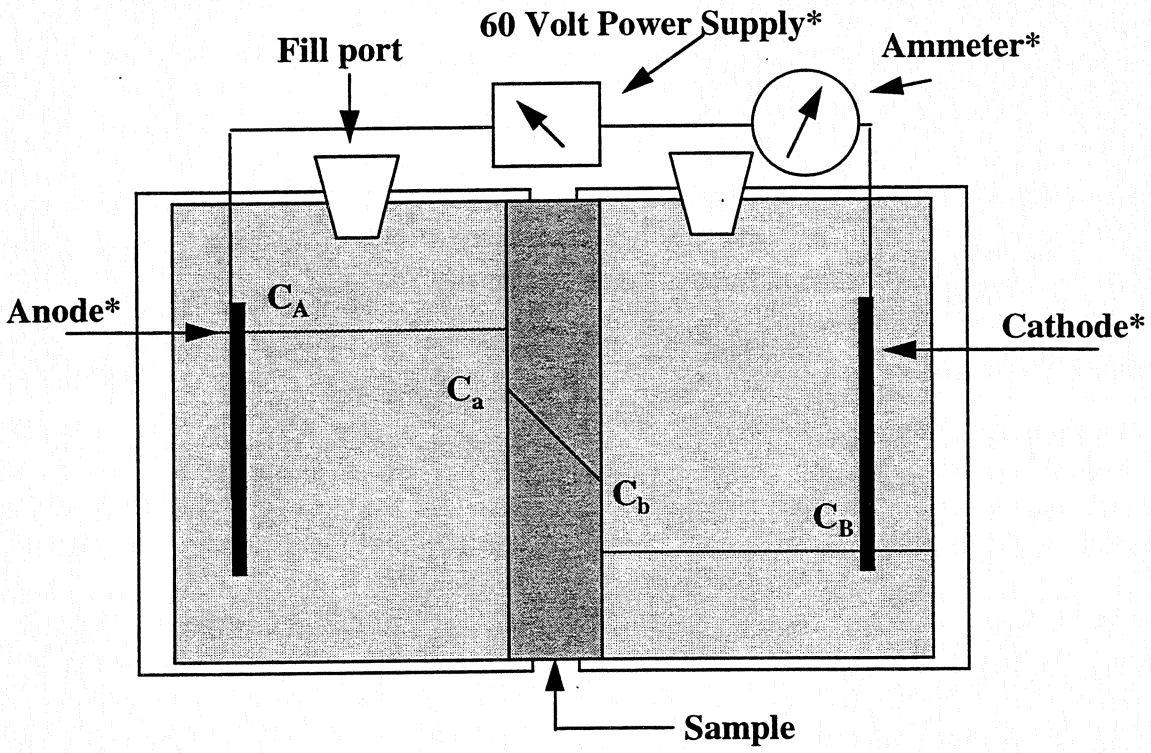


FIGURE 2 A schematic diagram for the apparatus used in the divided diffusion cell, rapid chloride permeability, and modified chloride permeability tests. *In the case of the divided diffusion cell, the power supply, electrodes, and ammeter are not used.

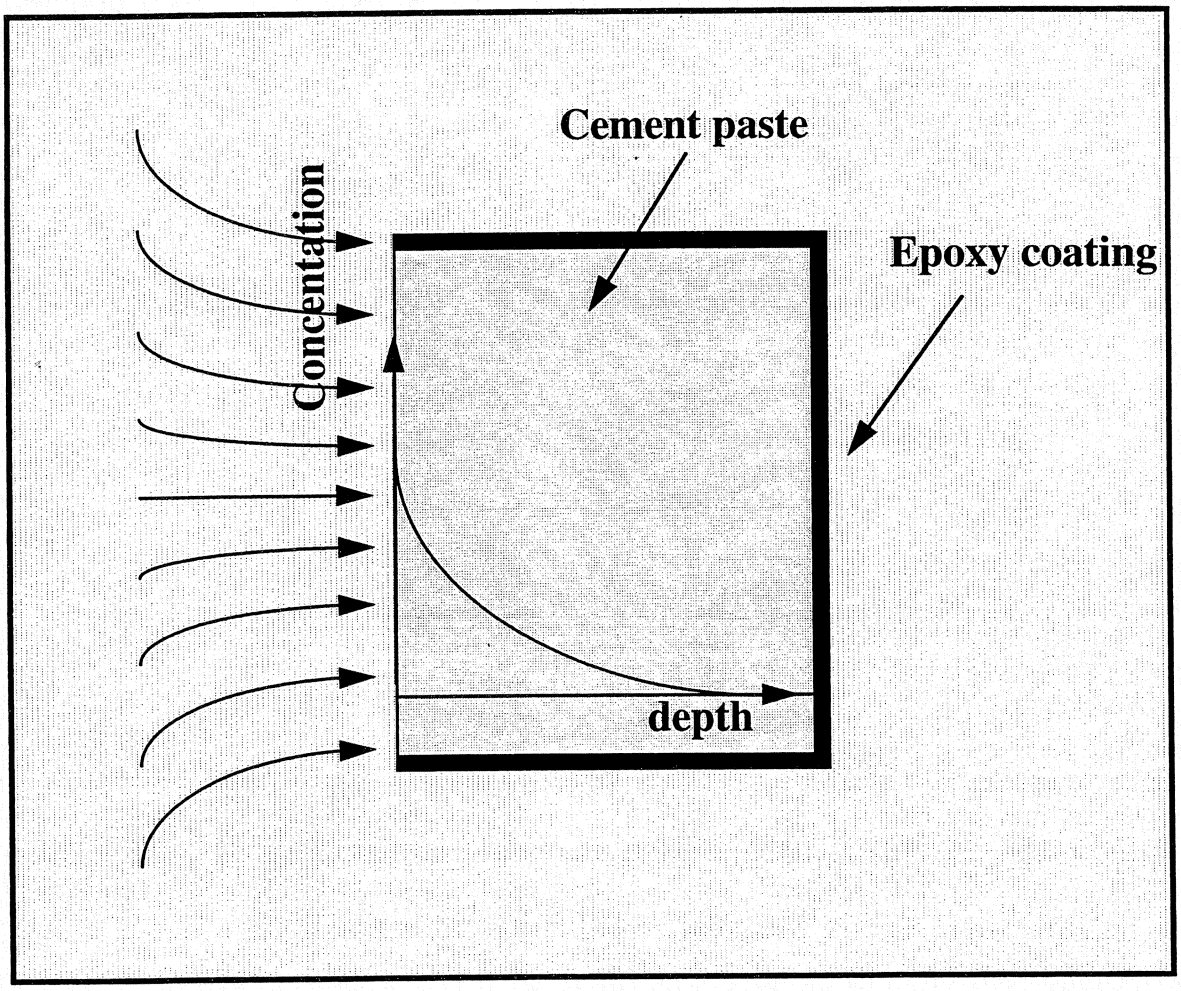


FIGURE 3 A schematic diagram of the ponding immersion experiment.

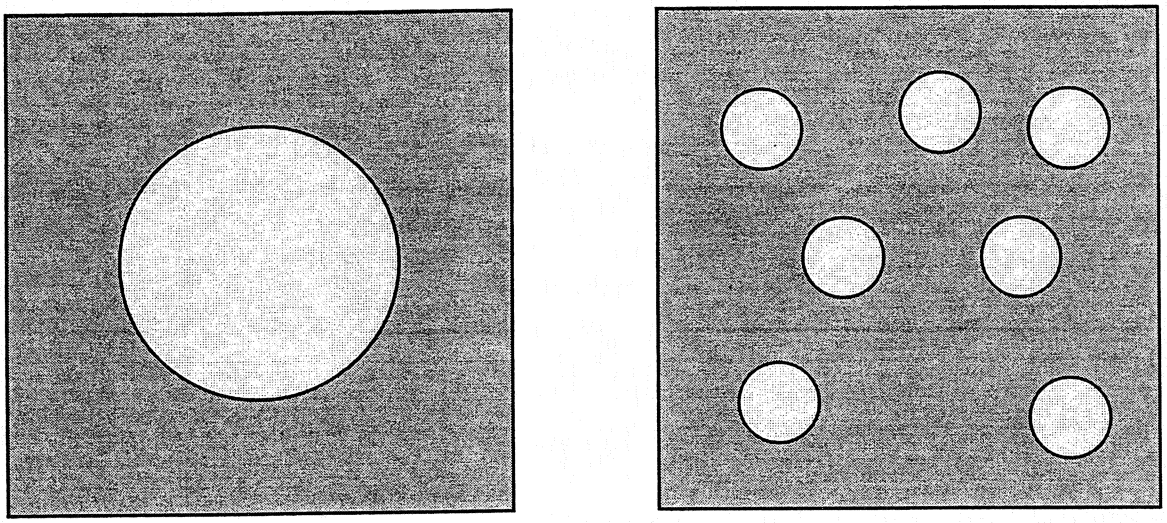


FIGURE 4 An idealized schematic of two pore structures with equal porosity, but different pore diameters.

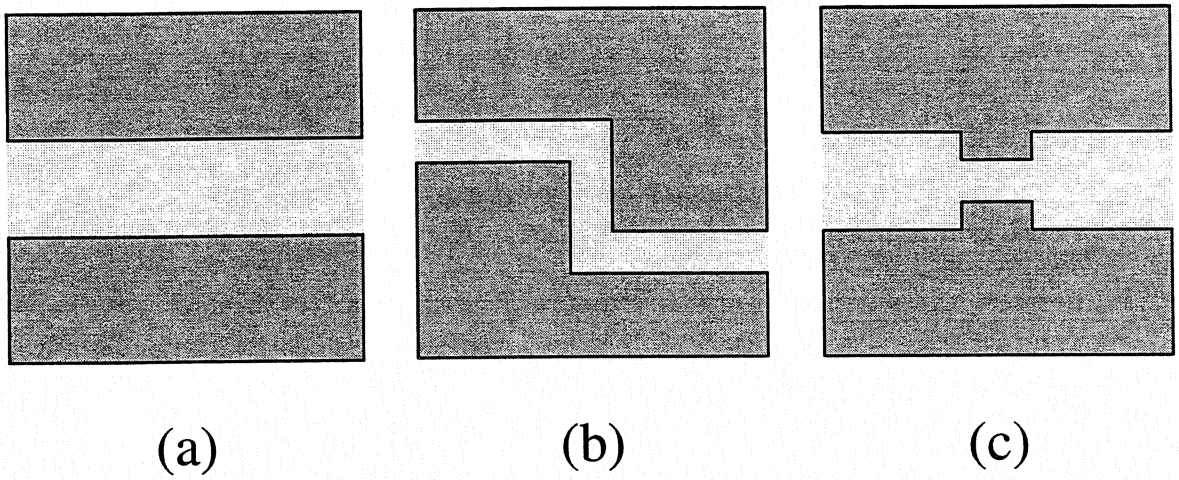


FIGURE 5 Idealized schematics of three pores of identical volume, where (a) has a connectivity (β) equal to one and (b) and (c) have connectivities (β) less than one owing to either: (a) a longer pathlength or (b) a constriction of the pore.

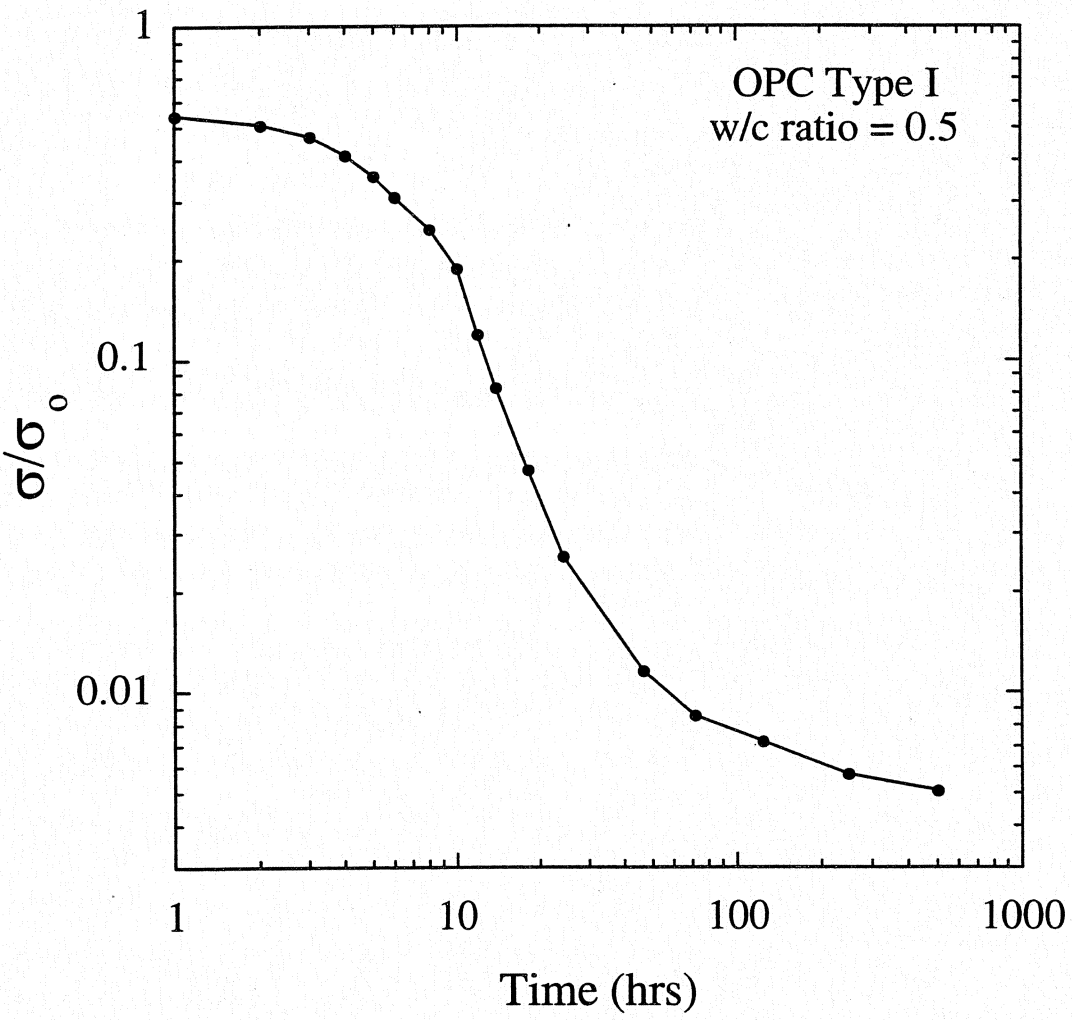


FIGURE 6 Normalized conductivity versus time for a neat portland cement paste, water:cement ratio = 0.50.

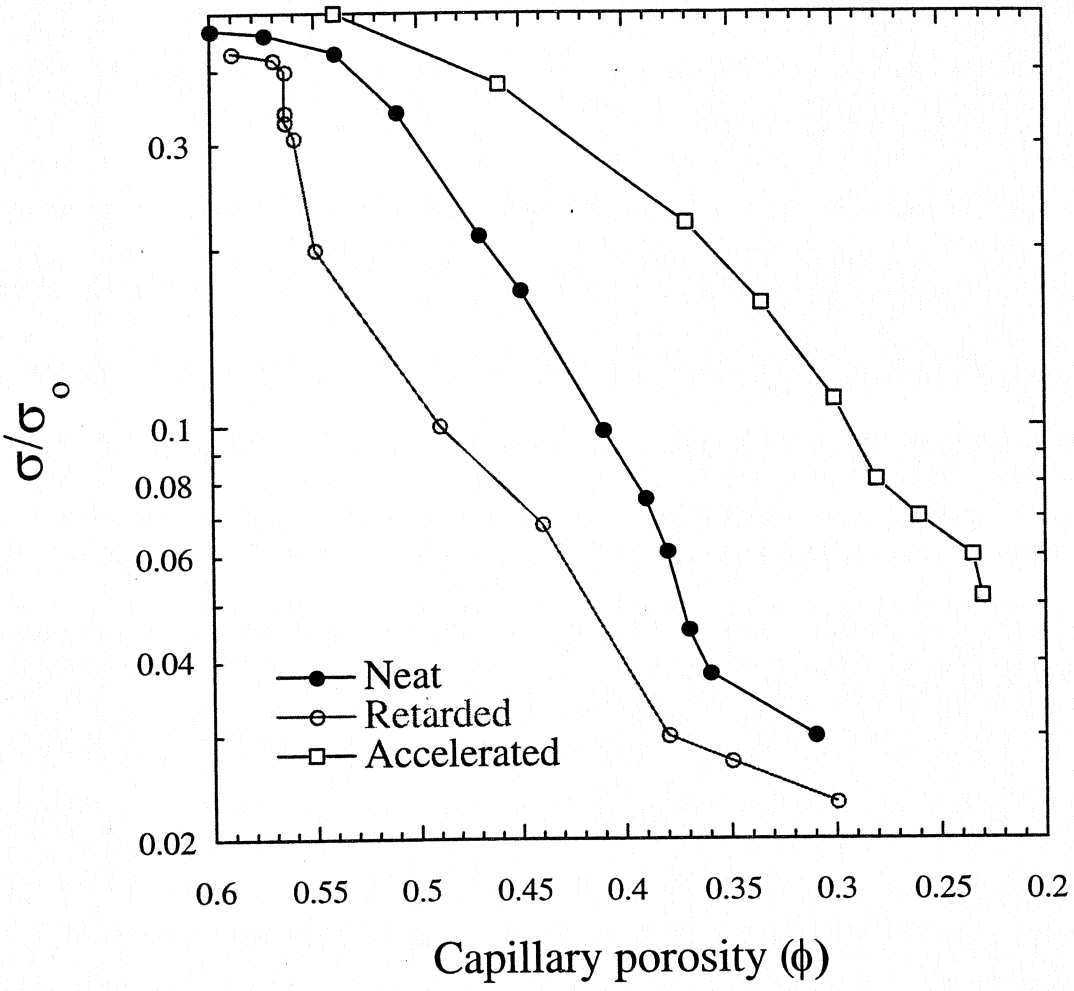


FIGURE 7 The normalized conductivity as a function of capillary porosity for a neat cement paste, a paste accelerated with $CaCl_2$, and a paste retarded with sucrose (used with permission of the publisher) (*13*).

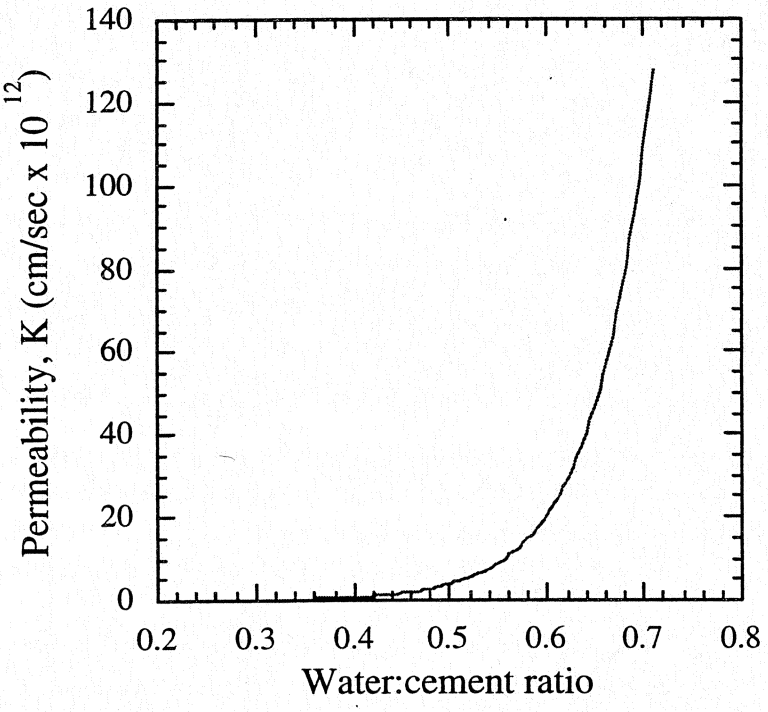


FIGURE 8 The effect of the water:cement ratio on the permeability of neat cement pastes hydrated near maximum hydration (adapted from (*18*)).

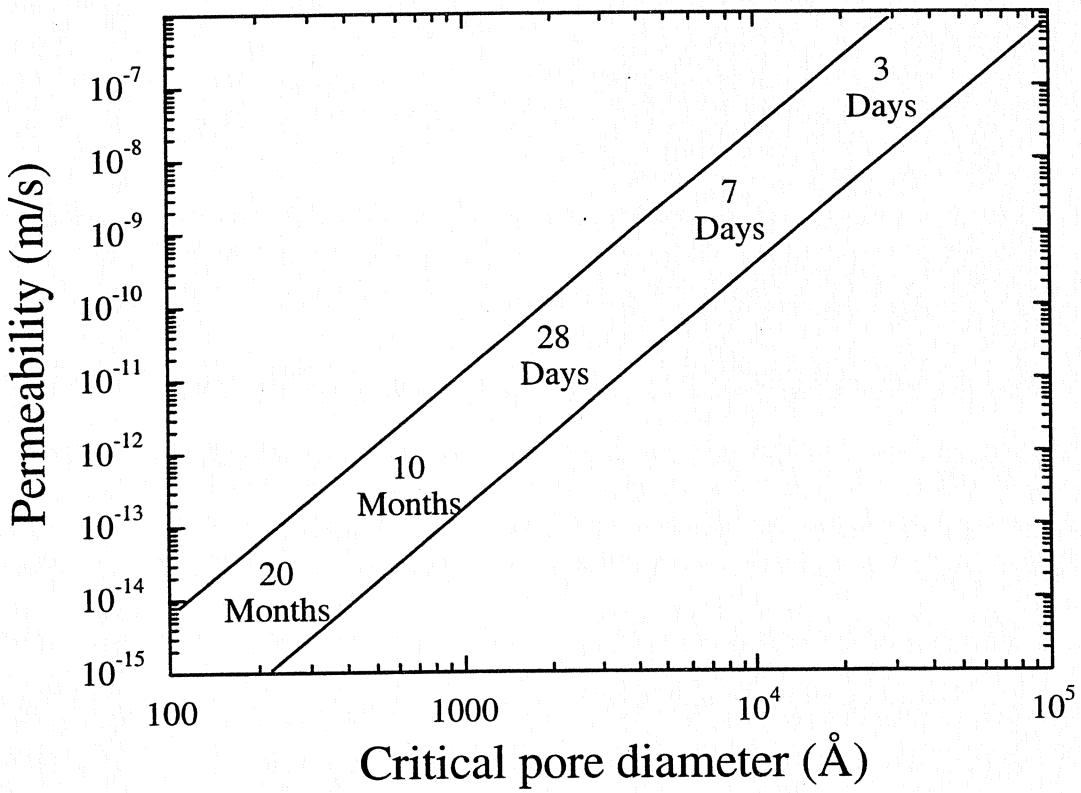


FIGURE 9 Influence of critical pore diameter on hydraulic permeability (adapted from (*19*)). The time labels give the approximate critical pore diameter and permeability for cement-pastes of that age.

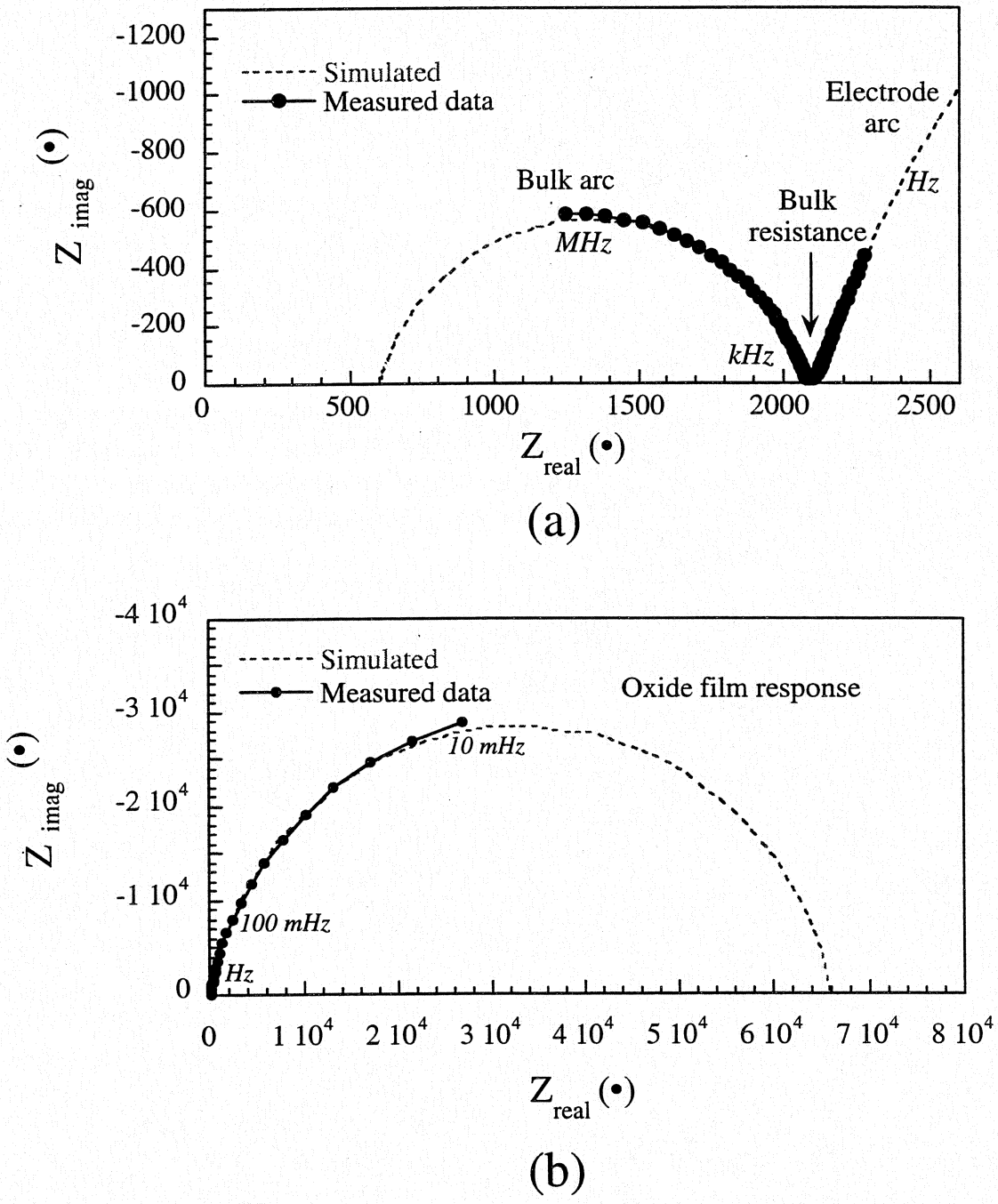


FIGURE 10 A typical Nyquist plot for a type I ordinary portland cement paste showing the (a) bulk response and (b) oxide film response. (the data is for a 14 day old paste with a water:cement ratio = 0.40). The dashed lines are simulated data based on equivalent circuit modelling.

REFERENCES

1. Transportation Research Board, National Academy of Science, 1986.

2. Mangat, P.S., J.M. Khatib & B.T. Molloy. Microstructure, Chloride Diffusion and Reinforcement Corrosion in Blended Cement and Concrete *Cement and Concrete Composites,* Vol. 16, No. (1994) pp. 73-81.

3. Mindess, S. & J.F. Young. *Concrete*. Prentice Hall, Inc., Englewood Cliffs, NJ, 1981.

4. Taylor, H.F.W. *Cement Chemistry*. Academic Press, San Diego, 1990.

5. Jennings, H.M. & P.D. Tennis. Model for the Developing Microstructure in Portland Cement Pastes *Journal of the American Ceramic Society,* Vol. 77, No. 12, (1994) pp. 3161-3172.

6. MacDonald, K.A. & D.O. Northwood. Experimental Measurement of Chloride Ion Diffusion Rates Using a Two-Compartment Diffusion Cell: Effects of Material and Test Variables *Cement and Concrete Research,* Vol. 25, No. 7, (1995) pp. 1407-1416.

7. ASTM-C1202-91. Standard Test Method for Electrical Indications of Concrete's Ability to Resist Chloride Penetration in *American Society for Testing and Materials.* Philadelphia, 1991

8. Haque, M.N. & O.A. Kayyali. Free and Water Soluble Chloride in Concrete *Cement and Concrete Research,* Vol. 25, No. 3, (1995) pp. 531-542.

9. Detwiler, R.J., K.O. Kjellson & O.E. Gjorv. Resistance to Chloride Intrusion of Concrete Cured at Different Temperatures *ACI Materials Journal,* Vol. 88, No. 1, (1991) pp. 19-24.

10. Atkinson, A. & A.K. Nickerson. The Diffusion of Ions Through Water-Saturated Cement *Journal of Materials Science,* Vol. 19, No. (1984) pp. 3068-3078.

11. Garboczi, E.J. Permeability, Diffusivity, and Microstructural Parameters: A Critical Review *Cement and Concrete Research,* Vol. 20, No. 4, (1990) pp. 591-601.

12. Bockris, J.O. & A.K.N. Reddy. *Modern Electrochemistry*. Plenum Press, New York, 1979.

13. Christensen, B.J. Ph.D. Thesis, Northwestern University, 1993

14. Mehta, P.K. Sulfate Attack on Concrete - A Critical Review in *Materials Science of Concrete III.* (ed. Skalny, J.) The American Ceramic Society, Westerville, OH, 1992 pp. 105-131

15. Hansson, C.M. Concrete: The Advanced Material of the 21st Century *Metallurgical and Materials Transactions A,* Vol. 26A, No. (1995) pp. 1321-1341.

16. Banthia, N. & S. Mindess. Water Permeability of Cement Paste *Cement and Concrete Research,* Vol. 19, No. 5, (1989) pp. 727-736.

17. Katz, A.J. & A.H. Thompson. Quantitative Prediction of Permeability in Porous Rock *Physical Review B,* Vol. 34, No. 11, (1986) pp. 8179-8181.

18. Powers, T.C., L.E. Copeland, J.C. Hayes & H.M. Mann. Permeability of Portland Cement Paste *Journal of the American Concrete Institute,* Vol. 26, No. 3, (1954) pp. 285-298.

19. Nyame, B.K. & J.M. Illston. in *Seventh International Conference on the Chemistry of Cement* Paris, France, 1988 pp. 181-185

20. Ollivier, J.P. & M. Massat. Permeability and Microstructure of Concrete: A Review of Modelling *Cement and Concrete Research,* Vol. 22, No. 2/3, (1992) pp. 503-514.

21. Gau, Y. & I. Cornet. Permeability, Diffusivity and Microstructural Parameters *Corrosion,* Vol. 41, No. (1985) pp. 93-100.

22. Goto, S. & D.M. Roy. The Effect of W/C Ratio and Curing Temperature on the Permeability of Hardened Cement Paste *Cement and Concrete Research,* Vol. 11, No. 4, (1981) pp. 575-579.

23. Halamickova, P., R.J. Detwiler, D.P. Bentz & E.J. Garboczi. Water Permeability and Chloride Ion Diffusion in Portland Cement Paste Mortars: Relationship to Sand Content and Critical Pore Diameter *Cement and Concrete Research,* Vol. 25, No. 4, (1995) pp. 790-802.

24. Ollivier, J.P., J.C. Maso & B. Bourdette. Interfacial Transition Zone in Concrete *Journal of Advanced Cement Based Materials,* Vol. 2, No. (1995) pp. 30-38.

25. Ozyildirim, C. Laboratory Investigations of Low-Permeability Concretes Containing Slag and Silica Fume *ACI Materials Journal,* Vol. 91, No. 2, (1994) pp. 197-202.

26. Christensen, B.J., *et al.* Impedance Spectroscopy of Hydrating Cement-Based Materials: Measurement, Interpretation, and Application *Journal of the American Ceramic Society,* Vol. 77, No. 11, (1994) pp. 2789-804.

27. Ford, S.J. & T.O. Mason. in *Techniques to Assess the Corrosion Activity of Steel Reinforced Concrete Structures, ASTM STP 1276* (eds. Berke, N.S., Escalante, E., Nmai, C.K. & Whiting, D.) American Society for Testing and Materials, Philadelphia, PA, 1995.

28. Whiting, D. Rapid Measurement of the Chloride Permeability of Concrete *Public Roads,* Vol. 45, No. 3, (1981) pp. 101-112.

ACKNOWLEDGMENTS

This work was supported by the National Science Foundation through the Science and Technology Center for Advanced Cement-Based Materials under grant DMR-91-20002. The authors would also like to gratefully acknowledge Steven Ford for his beneficial advice and discussions.